The Journal of National Chiao Tung University
Vol. I, April 1976
pp.133-154

氮化硼－矽介面之電氣特性

Electrical Characteristics of the Boron Nitride-Silicon Interface

吳啓明 **Chii-Ming Wu**
Institute of Electronics

吳慶源 **Ching-Yuan Wu**
Department of Electronics Engineering

(Received January 23, 1976)

ABSTRACT — Boron nitride thin films on silicon substrate were prepared by electron-beam evaporation techniques for wide range of substrate temperature control and different tempeature nitriding annealing processes. It is found that the interface charge of boron nitride thin film on silicon gives the negative surface state charge of $2.5x10^{11}/cm^2$ and $7.6x10^{11}/cm^2$ for n- and p-type silicon substrate, respectively, the flat-band voltage is always less than one volt. The surface state density of MIS capacitor structure is studied by the differentiation method, and the trapped charge rearrangements due to B-T testing are interpreted. The boron nitride thin film properties are also studied by I-V characteristics. It is found that the precipitates of B_2O_3 will give the ohmic conduction current with activation energy of 0.395 ev for n-type sample at low positive gate voltage (electric field less than 10^4v/cm), the Schottky emission conduction rather than the Frenkel-Poole emission is observed at high electric field (>10^4v/cm) for both n- and p-type silicon MIS capacitor structure. The boron nitride p- and n-channel MISFET are fabricated by using the conventional planar technology incorporated with the electron-beam evaporation of boron-nitride gate insulator layer. The electrical properties and possible device applications are examined.

I. Introduction

Boron nitride is an exceptionally inert refractory compound, it has a unique combination of properties which has made it valuable both as an engineering and an electronic material. The crystalline boron nitride, generally, has two phases, one has the hexagonal wurzite structure which is similar to that of graphite, the other has the cubic zinc-blende structure which is similar to that of diamond. The zinc-blende structure is always formed by high pressure compression at the temperature larger than 2000°C, and the hexagonal wurzite structure can be formed at room temperature and is considered as an III-V compound semiconductor or an insulator with energy gap of 3.8 ev. Boron nitride is a white, opaque, readily-machinable refractory, good resistant to thermal shock, chemical corrosion, and has relatively high heat conductivity and outstanding dielectric properties. In semiconducting III-V compound, it displays multi-band electro-, photo-, and cathode-ray luminescence. [1-3]

Thin film boron nitride properties and application are seldom published formally. Films less than 1μ thick had been prepared by Habereckt, et al.[4], and characterized as capacitor dielectrics, and also by Rand, et al. [5], and suggested to be used as an semiconductor surface passivation material, boron diffusion source and thin film dielectric or varistor applications.

We report here the first results of a study of thin film boron nitride prepared by electron-beam evaporation technique. Boron nitride thin film on silicon deposited by the high energy electron beam evaporation technique is studied by the wide range of substrate temperature control and different temperature annealing processes. Electrical properties of boron nitride thin film are studied by utilizing the metal-insulator-semiconductor (MIS) capactior structure where the interface properties of boron nitride-silicon are examined by means of capacitance-voltage measurements and current-voltage relations. Boron-nitride p- and n-channel metal-insulator silicon field effect transistor are realized by using the conventional planar technology, and its electrical properties are also characterized and discussed.

II. Preparation of Boron Nitride Thin Film

The apparatus used for the deposition of boron nitride thin films by electron-beam technique is shown in Fig. 1. The distance between the evaporator source and wafer holder can be adjusted to give a desired uniform deposition, the substrate wafer can be back heated by a ring configuration of tungsten filaments with separate power control, the substrate temperature is then monitored by means of pt-pt: 10% Rh surface thermo-couple. Silicon wafers with doping concentration of $1.3\times10^{15}\,cm^{-3}$ n-type and $1.8\times10^{16}\,cm^{-3}$ p-type <100> orientation are chosen as the deposition substrate, the commercial available hot pressed boron-nitride wafer is used as the evaporation source. After the strict cleaning of the silicon substrate wafer and the boron nitride wafer, they are put into the vacuum system. The pressure is kept at 10^{-6} torr during the run.

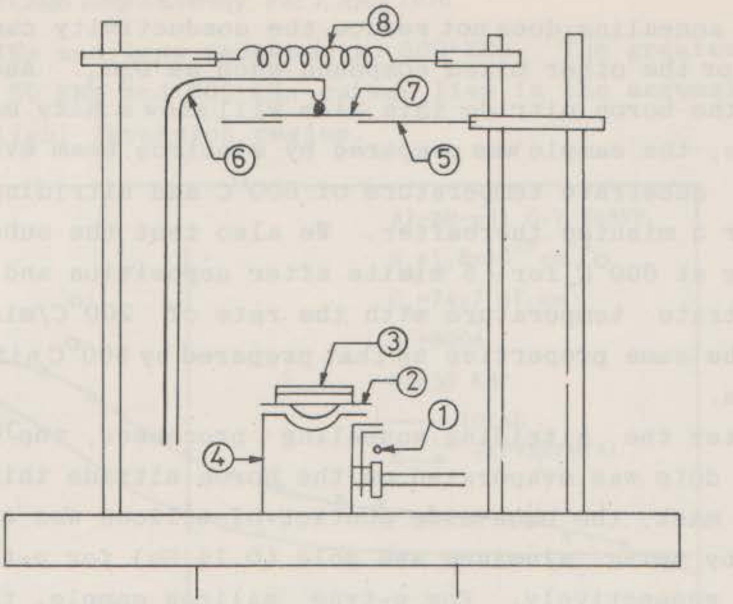

1. E-gun filament
2. Molybdenum target crucible
3. Evaporation material: boron nitride
4. Magnet and its water-cooling pipe
5. Substrate holder
6. Thermal couple used to monitor temperature
7. Substrate wafer
8. Tungsten substrate heating filament

Fig. 1. Schematic diagram of electron beam evaporation apparatus.

Since the hexagonal boron nitride has a small lattice constant ($a/\sqrt{3}$ =1.44 A^o, $C/\sqrt{2}$ =3.33A^o) in the hexagonal plane, which is much smaller than that of silicon, hence adhesion will be the main problem in the device engineering. Room temperature substrate deposition will produce a poor adhesion of boron nitride film on silicon, the deposited boron nitride film can even be rinsed out by deionized water. Therefore,the constant substrate temperature above the room temperature is required to insure the good adhesion and quality in sample preparations. In this report, the substrate temperature was kept at 600^{o}C, and nitriding annealing condition is tested at temperature ranged from 400^{o}C to 1200^{o}C with annealing time ranged from 5 minutes to 80 minutes. It is found that long-time annealing causes the sample color deeper and thinner, typically 20%, which appeared to be larger in crystalline size, but the interface surface states are increased due to more vacancy involved. Low temperature annealing does not reduce the conductivity caused by the impurities or the other mixed compound such as B_2O_3. Above 900°C annealing the boron nitride thin film will show a hazy ceramic phase. Therefore, the sample was prepared by electron beam evaporation with constant substrate temperature of 600°C and nitriding annealing at 800°C for 5 minutes thereafter. We also test the subsequent vacuum annealing at 600°C for 5 minite after deposition and then lowering the substrate temperature with the rate of 200°C/min. The sample showed the same properties as that prepared by 800°C nitriding anneal-condition.

After the nitriding annealing processes, the 6000A° thick aluminum dots was evaporated on the boron nitride thin film through Mo metal mask, the back side contact of silicon was separately evaporated by using aluminum and gold (0.1% Sb) for p-type and n-type silicon, respectively. For p-type silicon sample, the Al metallization was sintered at 540°C in forming gases flowing embient for 5 minutes. For n-type silicon sample, the metallization of Al and Au (0.1% Sb) was separately sintered at 540°C and 370°C for 5 minutes after each metallization step. After finishing the above stated processes, the sample was scribed and mounted on TO-5 header for package, then capacitance-voltage and current-voltage characteristics were measured.

III. Electrical Properties and Measurements

1. C-V Characteristics

The interface properties of a MIS capacitor structure are always measured from the C-V characteristics. The room temperature capacitance-voltage and conductance-voltage are simultaneous measured by BEC 74 capacitance bridge in which the measured frequency can' range from 5 KHz to 500 KHz. In these frequency ranges, the conductance method for calculating the surface state density is not available, but the time constant of the fast surface state will be larger than 5 msec. The surface charge number is calculated by comparing the experimental C-V curves with the ideal C-V curves.

For p-type substrate sample, the C-V curves showed the presence of fast surface states as is shown in Fig. 2. For this sample the flat-band voltage is always less than 1 volts for frequency changed from 50 KHz to 500 Khz. A comparison of Fig. 2 shows, a difference in the energy position of the surface states which could strongly response to 50 KHz and less response to 500 KHz. The greatest difference between 50 KHz and 500 KHz curves lies in the accumulation, depletion and slight inversion region.

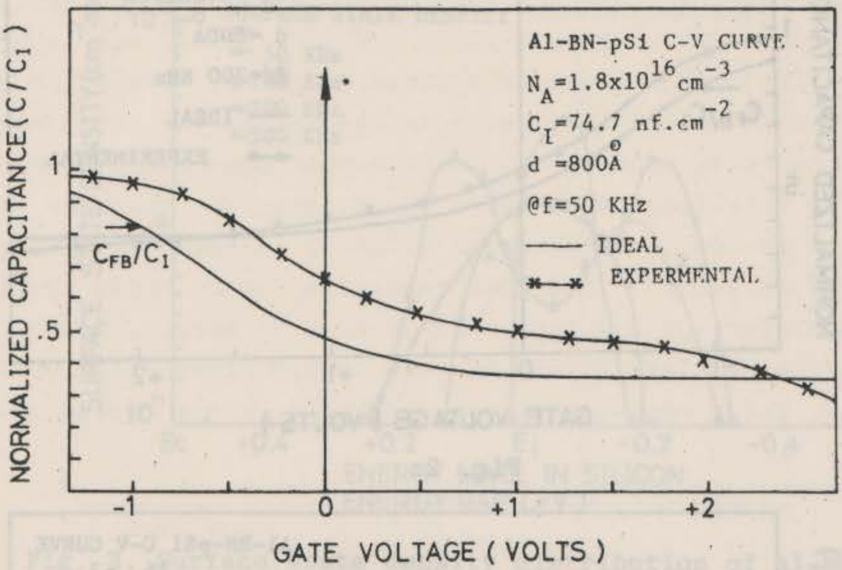

Fig. 2a

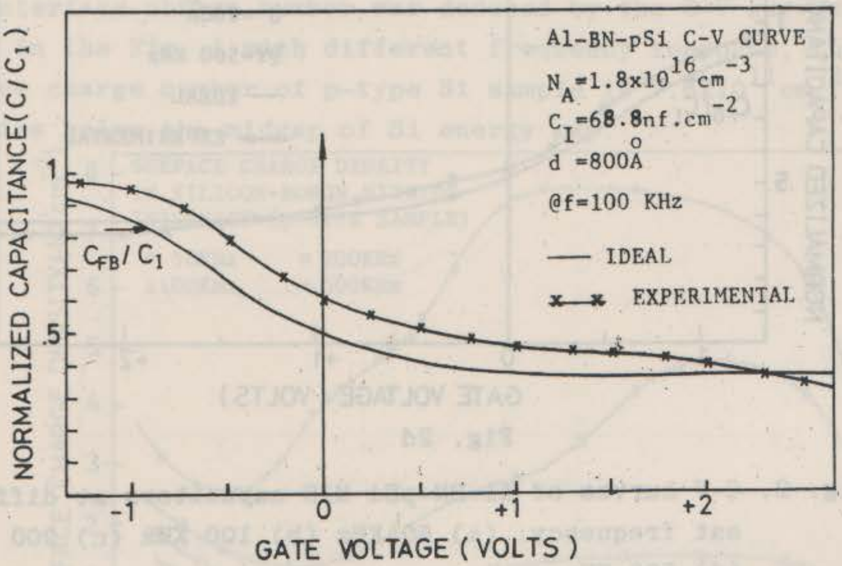

Fig. 2b

This indicates that, where as the fastest states lie near the energy midgap, and frequency of 500 KHz was sufficiently high to freeze out the most of surface states.

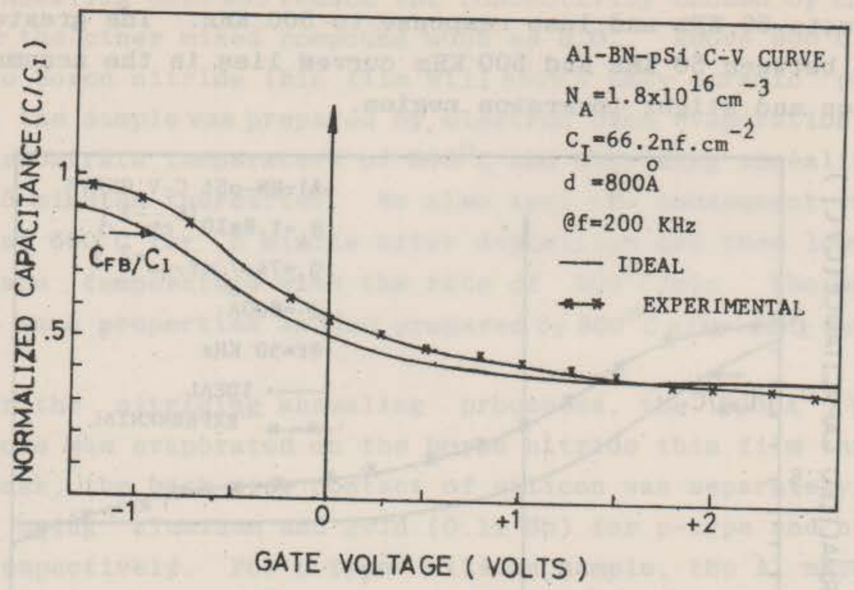

Fig. 2c

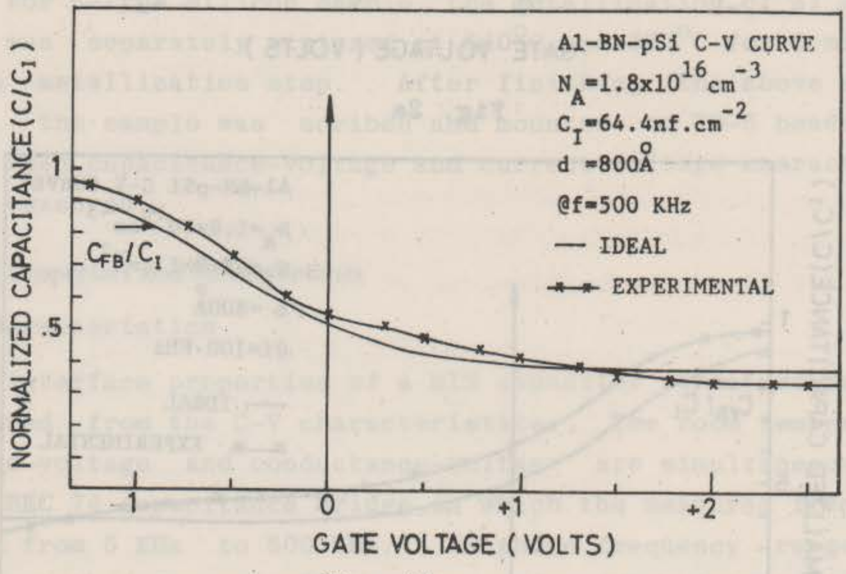

Fig. 2d

Fig. 2. C-V curves of Al-BN-pSi MIS capacitors at different frequency: (a) 50 KHz (b) 100 KHz (c) 200 KHz (d) 500 KHz.

The surface state energy distribution was calculated by differentiation method, and was shown in Fig. 3, the maximum surface state density is $3.3\text{x}10^{12}\ \text{cm}^{-2}\ \text{ev}^{-1}$ at approximate middle of energy gap. The flat band voltage of Fig. 2 also showed that the C-V curves are always shifted toward the positive gate voltage axis by comparing with the ideal C-V characteristics which incluses the correction of work function difference. This positive voltage shifting means that the interface charge is negative for boron nitride-Si(p) MIS structure.

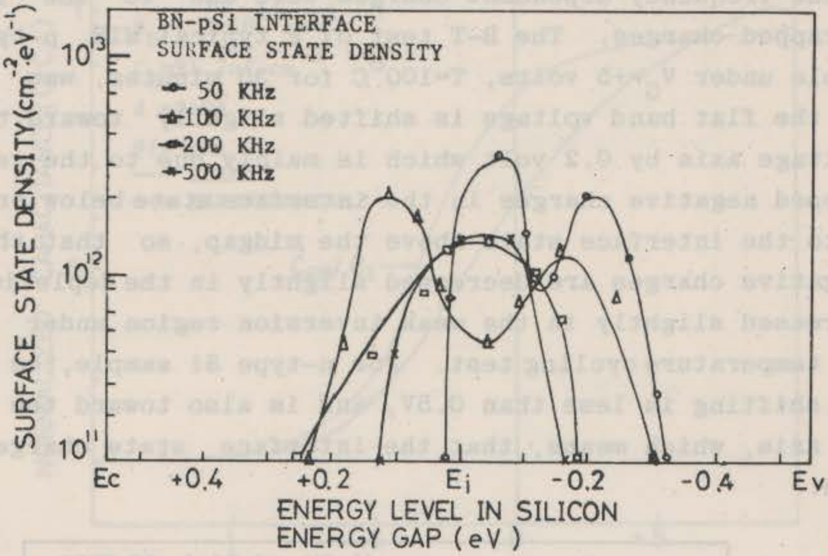

Fig. 3. Surface state density distribution of Al-BN-pSi MIS structure at different frequency.

The interface charge number was deduced by the C-V curves and was shown in the Fig. 4 with different frequency response, the maximum surface charge number of p-type Si sample is 7.6×10^{11} cm^{-2} at 50 KHz and lies below the midgap of Si energy gap.

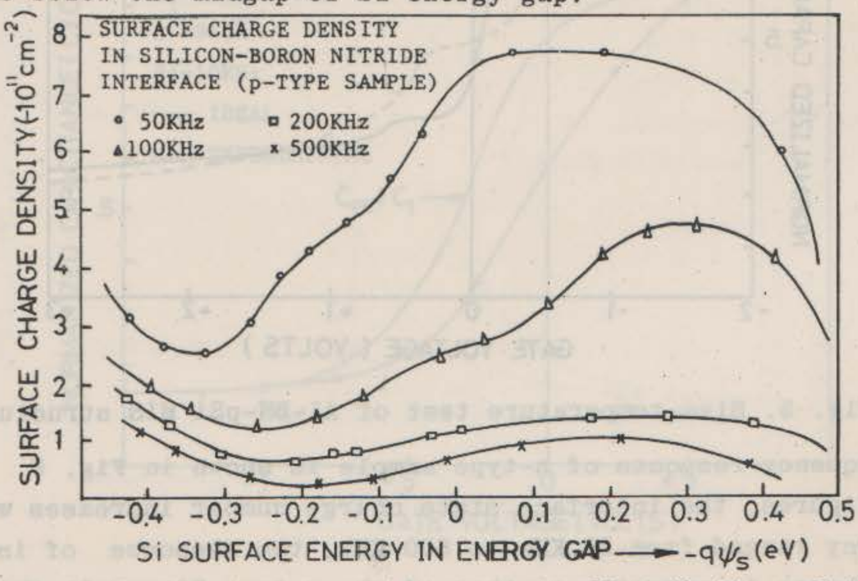

Fig. 4. Surface charge number energy distribution of Al-BN-pSi MIS structure at different frequency.

The surface charge number is dependent of frequency, which means that a very low fixed surface state charges as was shown at 500 KHz(~ 10^{11} cm^{-2}), the frequency dependent charges were due to the interface state trapped charges. The B-T test of a typical MIS p-type silicon sample under V_G=+5 volts, T=100°C for 35 minutes, was shown in Fig. 5, the flat band voltage is shifted slightly toward the negative voltage axis by 0.2 volt which is mainly due to the release of the trapped negative charges in the interface state below or near the midgap to the interface state above the midgap, so that the interface negative charges are decreased slightly in the depletion region, and increased slightly in the weak inversion region under positive voltage temperature cycling test. For n-type Si sample, the flat band voltage shifting is less than 0.5V, and is also toward the positive voltage axis, which means, that the interface state charge is also negative.

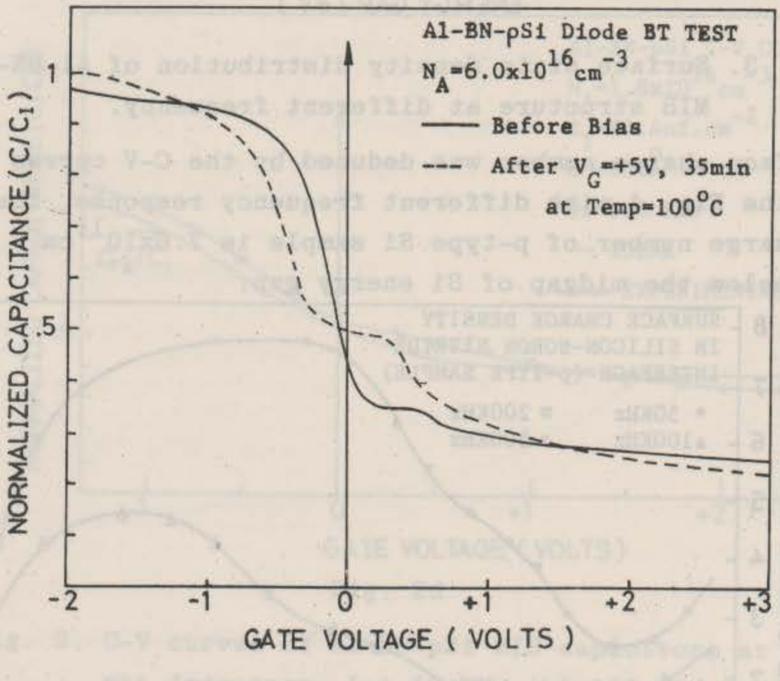

Fig. 5. Bias-temperature test of Al-BN-pSi MIS structure.

The frequency response of n-type sample is shown in Fig. 6. From these figures, the interface state charge number increases with the frequency ranged from 50 KHz to 500 KHz, the response of interface state charge is opposite to that of the p-type Si sample. The interface state energy distribution is shown in Fig. 7, the maximum interface state density is about $1.85 \times 10^{12} cm^{-2} ev^{-1}$ at 0.075 ev and 0.345 ev below the midgap for 50 KHz and 5 KHz, respectively.

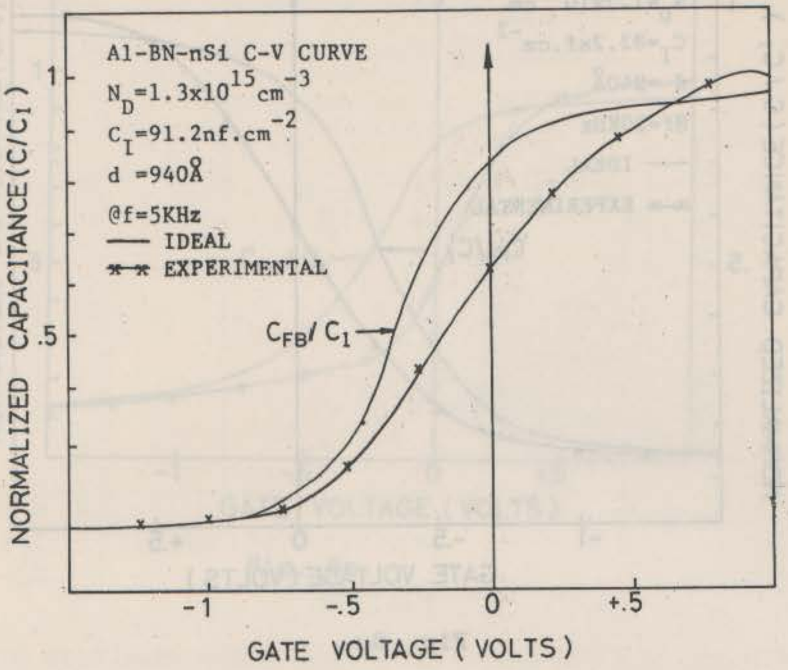

Fig. 6a.

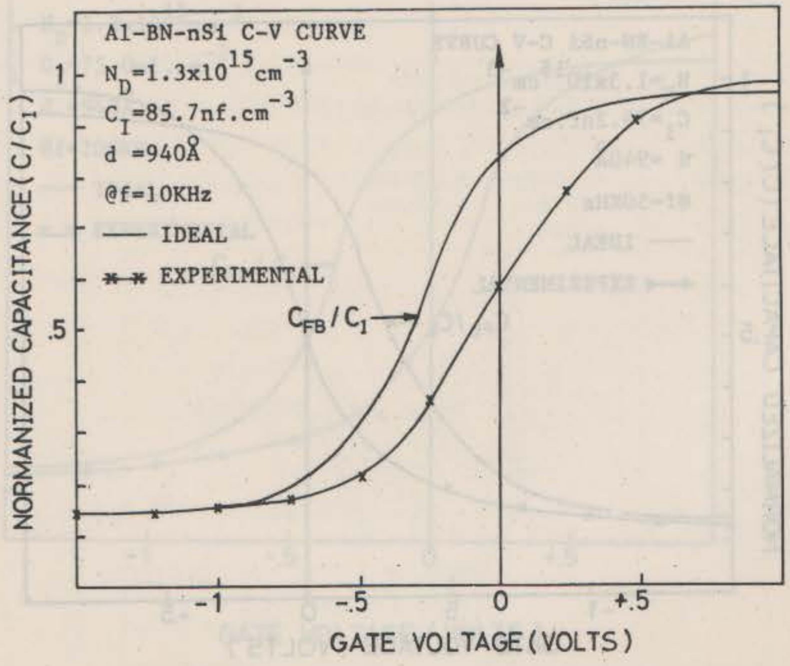

Fig. 6b.

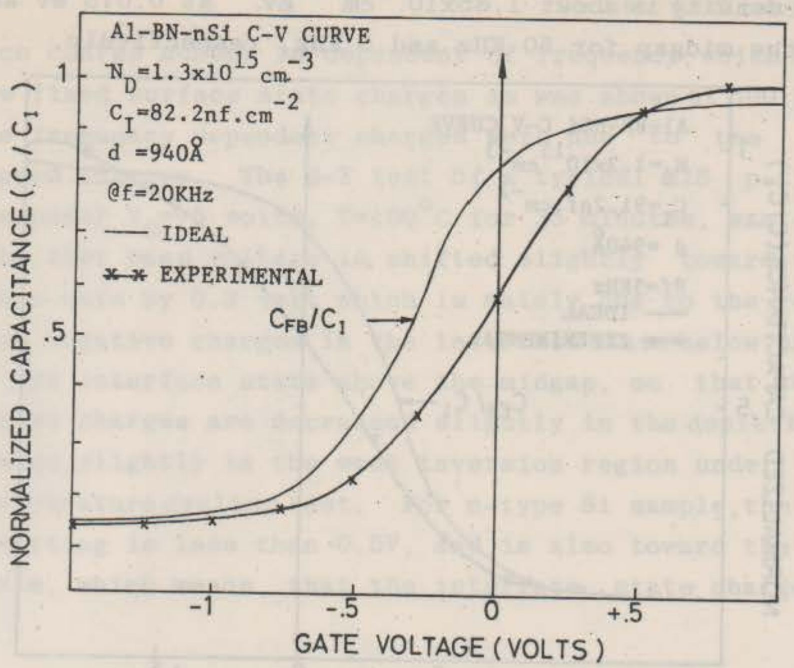
Al-BN-nSi C-V CURVE
N_D=1.3x10^15 cm^-3
C_I=82.2nf.cm^-2
d =940Å
@f=20KHz
IDEAL
EXPERIMENTAL
C_FB/C_I
NORMALIZED CAPACITANCE (C / C_I)
1
.5
-1
-.5
0
+.5
GATE VOLTAGE (VOLTS)

Fig. 6c.

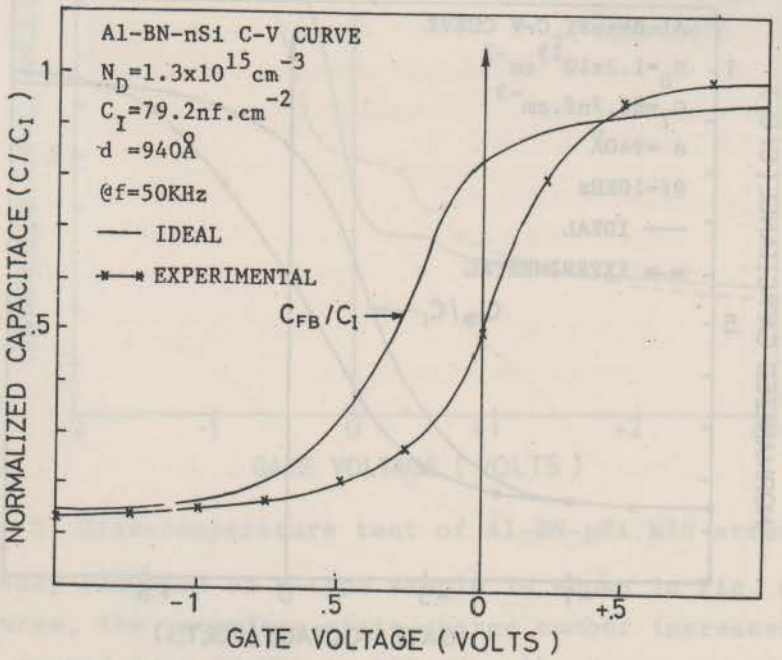
Al-BN-nSi C-V CURVE
N_D=1.3x10^15 cm^-3
C_I=79.2nf.cm^-2
d =940Å
@f=50KHz
IDEAL
EXPERIMENTAL
C_FB/C_I
NORMALIZED CAPACITACE (C/ C_I)
1
.5
-1
.5
0
+.5
GATE VOLTAGE (VOLTS)

Fig. 6d.

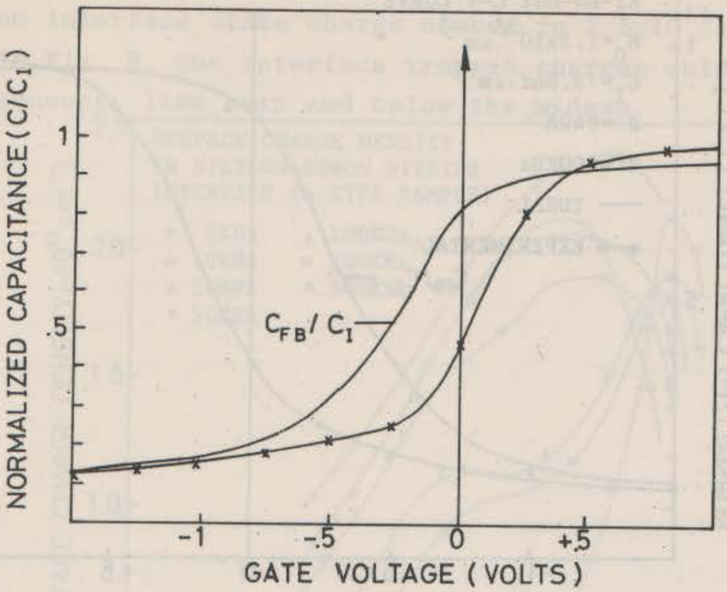
NORMALIZED CAPACITANCE (C/C_I)
1
.5
C_FB / C_I
-1
-.5
0
+.5
GATE VOLTAGE (VOLTS)

Fig. 6e.

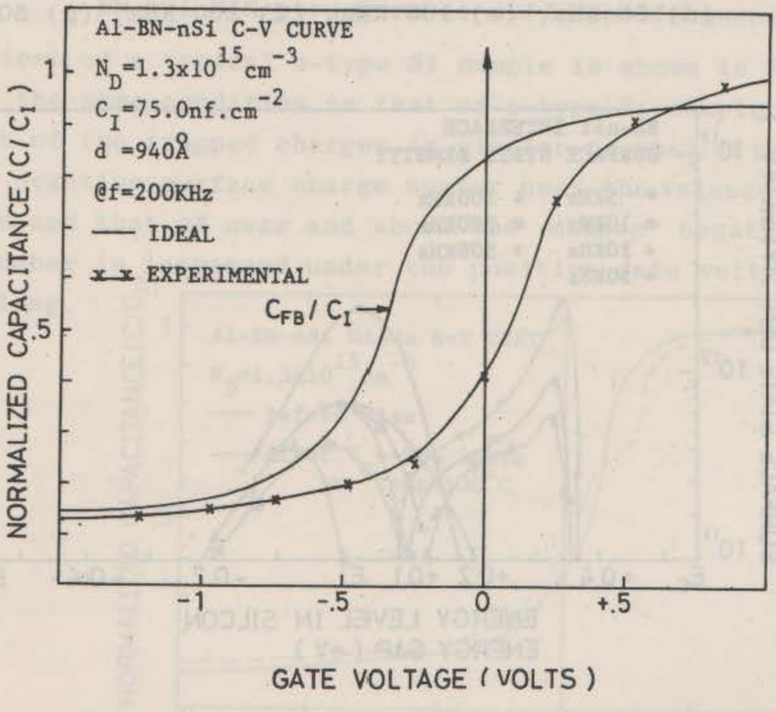
Al-BN-nSi C-V CURVE
N_D=1.3x10^15 cm^-3
C_I=75.0nf.cm^-2
d =940Å
@f=200KHz
— IDEAL
x–x EXPERIMENTAL
NORMALIZED CAPACITANCE (C/C_I)
1
.5
C_FB / C_I
-1
-.5
0
+.5
GATE VOLTAGE (VOLTS)

Fig. 6f.

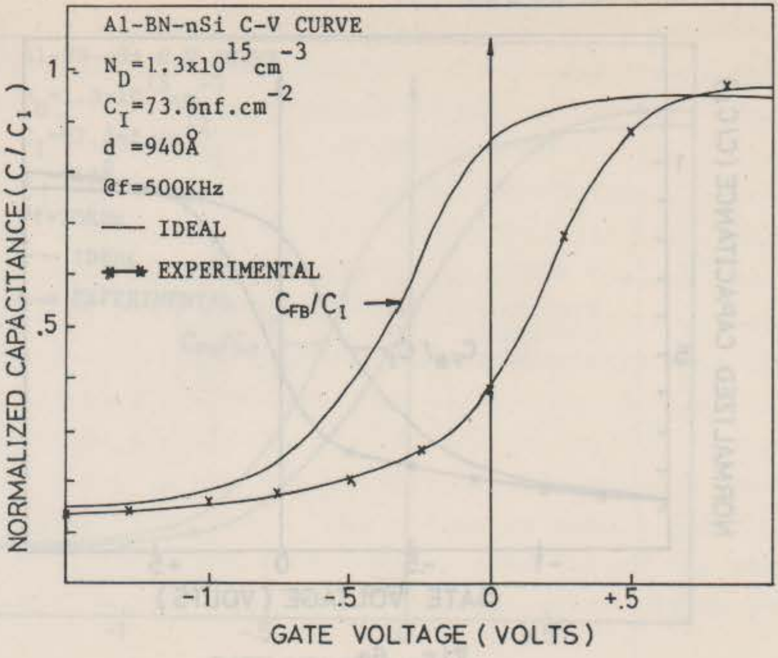

Fig. 6g.

Fig. 6. C-V curves of Al-BN-nSi MIS capacitors at different frequency: (a) 5KHz, (b) 10 KHz, (c) 20 KHz, (d) 50 KHz, (e) 100 KHz, (f) 200 KHz, (g) 500 KHz.

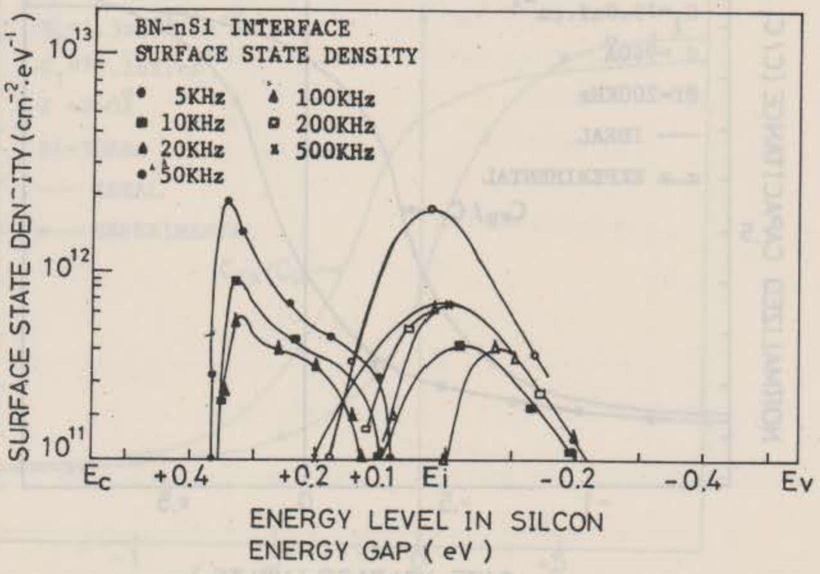

Fig. 7. Surface state density distribution of Al-BN-nSi MIS structure at different frequency.

The maximum interface state charge number is $2.5 \times 10^{11} cm^{-2}$ at 500 KHz as shown in Fig. 8, the interface trapped charges which can response to the frequency, lies near and below the midgap.

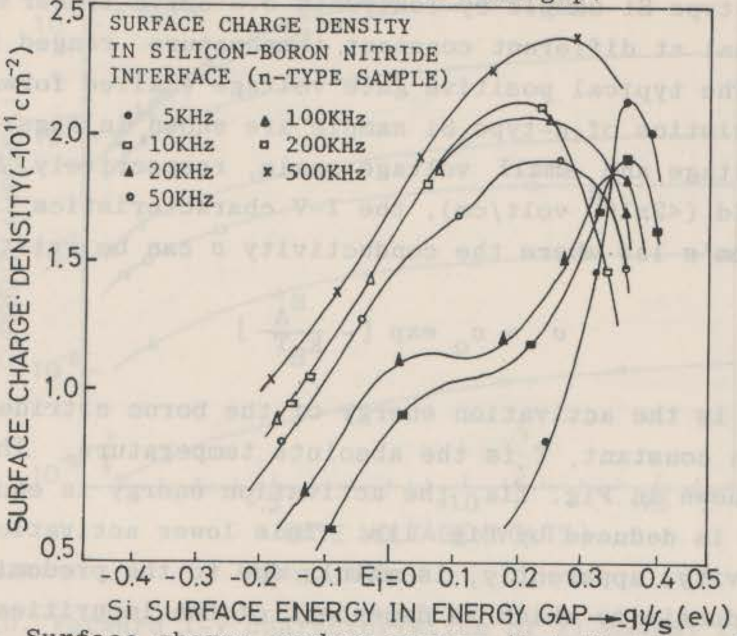

Fig. 8. Surface charge number energy distribution of Al-BN-nSi MIS structure at different frequency.

The B-T test of a typical n-type Si sample is shown in Fig. 9 which is under the same condition as that of p-type Si sample. The rearrangement of the trapped charges is similar to that of p-type Si sample, the negative surface charge number near the valence band edge is decreased and that of near and above the midgap negative surface charge number is increased under the positive gate voltage temperature cycling.

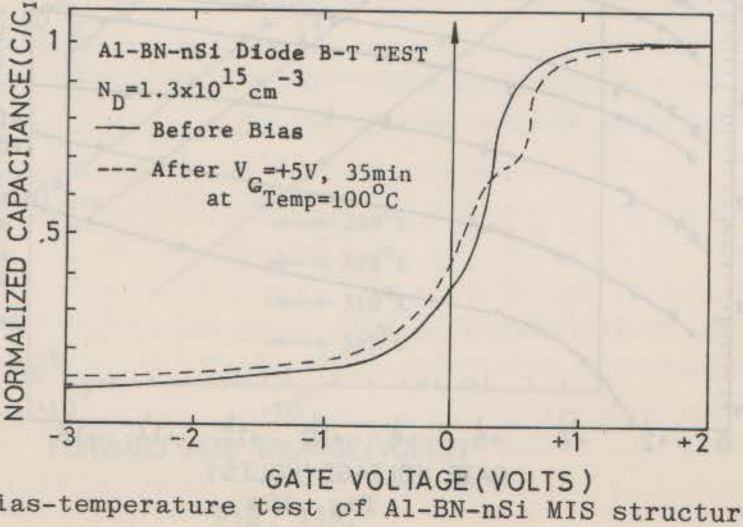

Fig. 9. Bias-temperature test of Al-BN-nSi MIS structure.

2. I-V characteristics

The I-V characteristics of MIS capacitor were measured for both n- and p-type Si sample by Tektronix 576 curve tracer with pulse voltage signal at different constant temperature ranged from -77°C to 157°C. The typical positive gate voltage (called forward bias) I-V characteristics of n-type Si sample are shown in Figs. 10 for both large voltage and small voltage scale, respectively. At lower electric field ($<2\times10^4$ volt/cm), the I-V characteristics is satisfied by the Ohm's law where the conductivity σ can be written as [6]

$$\sigma = \sigma_o \exp \left[- \frac{E_A}{k_B T}\right] \qquad (1)$$

where E_A is the activation energy of the boron nitride, k_B is the Boltzmann constant, T is the absolute temperature. The curve fitting is shown in Fig. 11a, the activation energy is equal to E_A=0.395 ev which is deduced by Fig. 11b. This lower activation energy of conductivity, apparently, is mainly due to the predominance of electron conductivity which is dependent of the impurities of B_2O_3. The activation energy of 0.395 will cause electrons in the impurity states activated by thermal energy and hopped motion from one isolated state to the next. This mechanism yields an ohmic characteristic exponentially dependent on temperature, which is similar to the case of Si_3N_4 insulator thin film on Si [7].

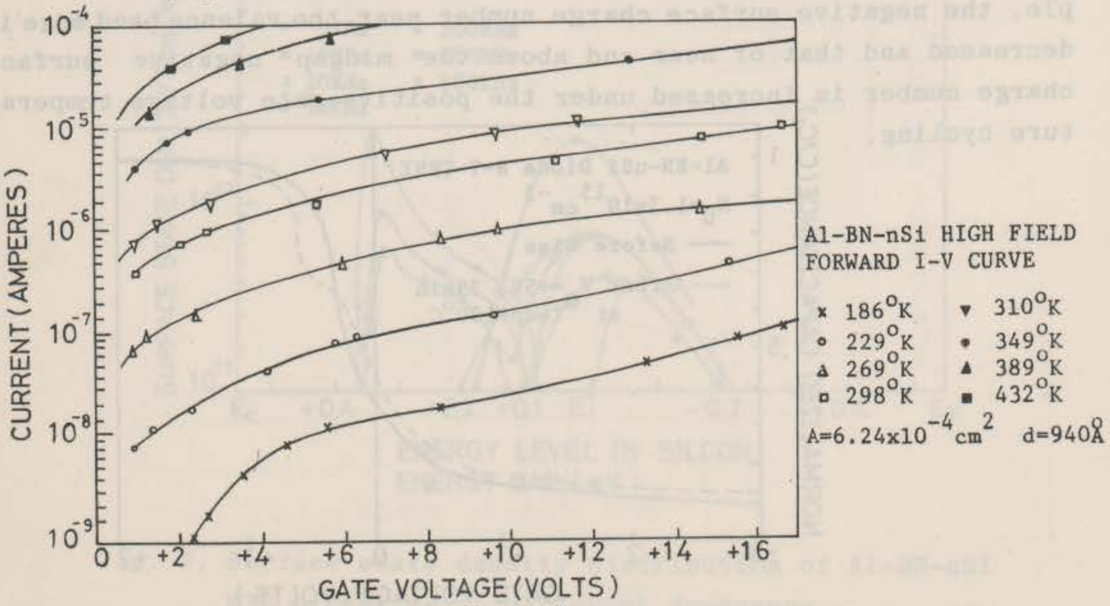

Fig. 10a.

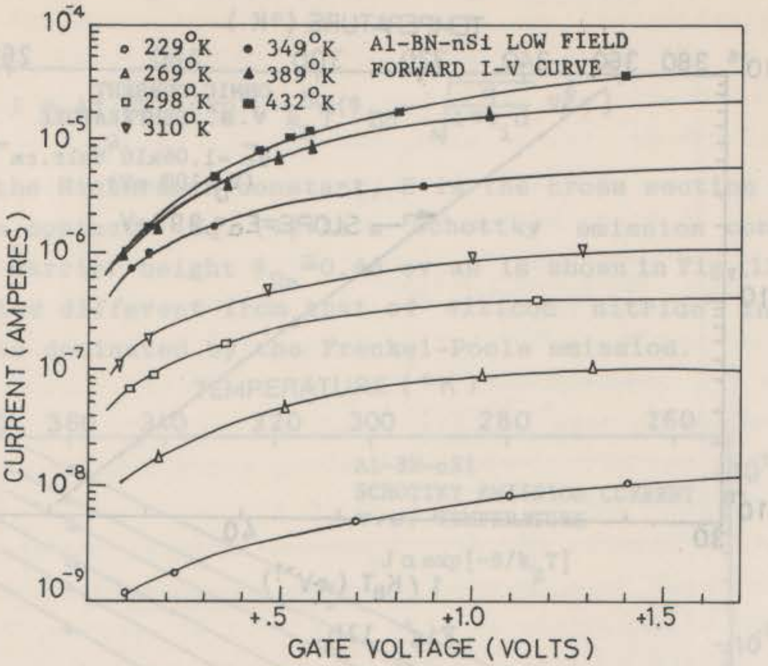

Fig. 10b.

Fig. 10. Forward I-V characteristics of Al-BN-nSi (a) high voltage range I-V curves, (b) low voltage range I-V curves.

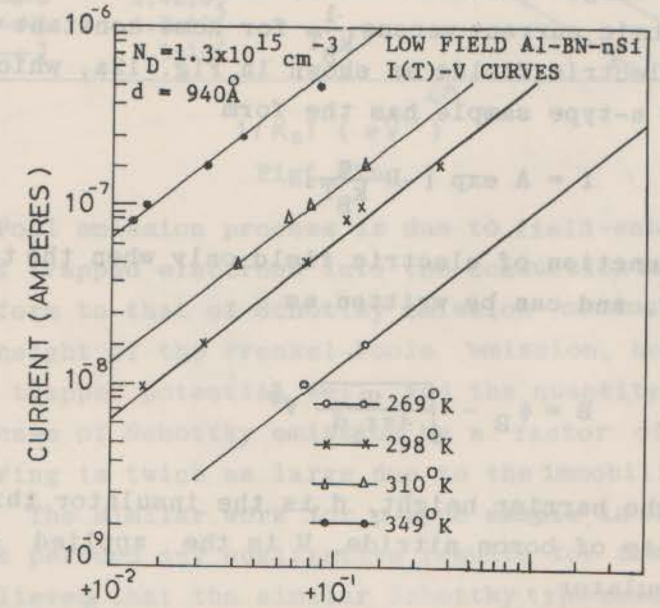

Fig. 11a.

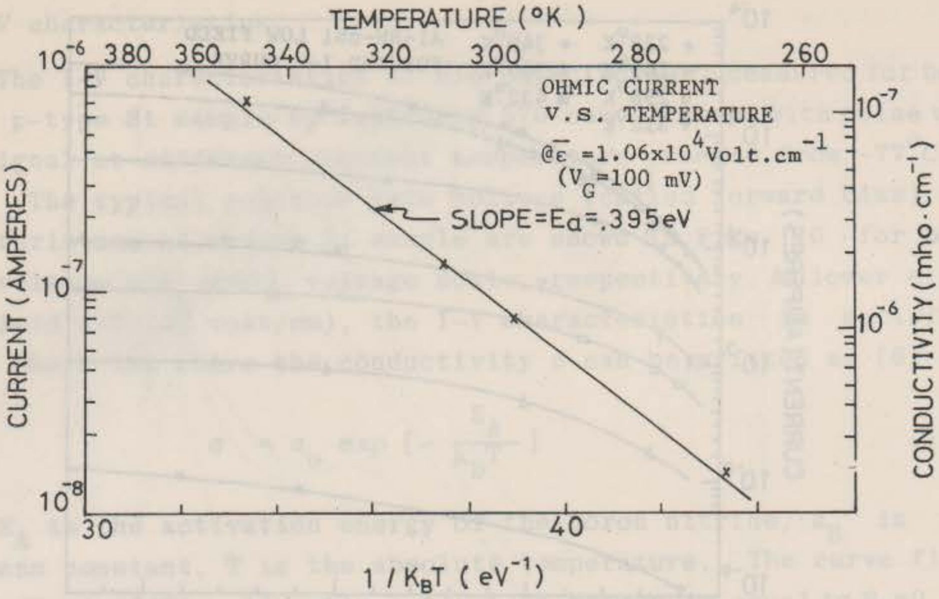

Fig. 11b.

Fig. 11. Low voltage range forward I-V characteristics of Al-BN-nSi (a) Log-Log plots, (b) Lot I v.s. $\frac{1}{k_BT}$ at constant voltage to deduce the ohmic region activation energy E_A.

For more larger electric field, the I-V characteristic is plotted in logarithmic current versus $\frac{1}{k_BT}$ for some constant voltages i.e., the constant electric fields as shown in Fig. 12a, which shows that the current of n-type sample has the form

$$I = A \exp\left[-B \frac{q}{k_BT}\right] \tag{2}$$

where B is a function of electric field only when the temperature is large than 0°C, and can be written as

$$B = \phi_B - \sqrt{\frac{q}{4\pi \varepsilon_i d}}\, V^{\frac{1}{2}} \tag{3}$$

where ϕ_B is the barrier height, d is the insulator thickness, ε_i is the permittivity of boron nitride, V is the applied gate voltage across the insulator.

When the electric field is larger than 3×10^5 volt/cm and ε_i is substituted by the value of $\varepsilon_i = 9.7\ \varepsilon_o$ which is the low frequency C-V measured data. The current-voltage characteristics can then be written as [7]

$$I = A^* ST^2 \exp\left[-\frac{q}{k_B T}\left(\phi_{Bn} - \sqrt{\frac{q}{4\pi\varepsilon_i d}}\, V^{\frac{1}{2}}\right)\right] \qquad (4)$$

where A* is the Richardson constant, S is the cross section area of metallization contact. Eq. (4) is a Schottky emission conduction current with barrier height $\phi_{Bn} \cong 0.46$ ev as is shown in Fig. 12b. The result is quite different from that of silicon nitride insulator layer which is dominated by the Frenkel-Poole emission.

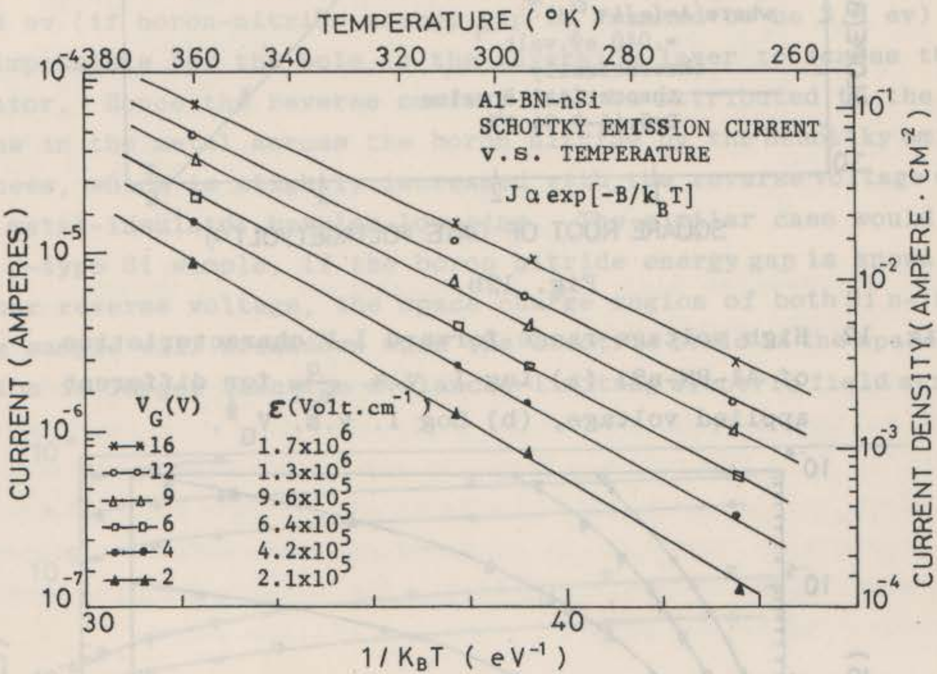

Fig. 12a.

The Frenkel-Pool emission process is due to field-enhanced thermal excitation of trapped electrons into the conduction band, which gives the similar form to that of Schottky emission conduction current. The barrier height of the Frenkel-Poole emission, however, is the depth of the trapped potential well, and the quantity $\sqrt{\frac{q}{\pi\varepsilon_i}}$ is larger than in the case of Schottky emission by a factor of 2 since the barrier lowering is twice as large due to the immobility of the positive charge. The similar work for p-type sample is shown in Fig. 13, which has not persued any qualitative results for its thinner film, but it is believed that the similar Schottky type emission will dominate the current transport.

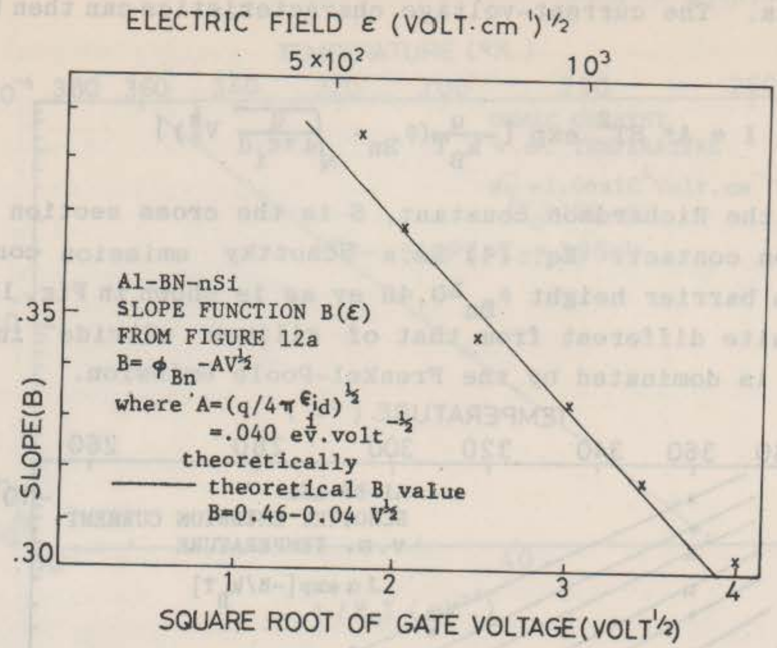

Fig. 12b.

Fig. 12. High voltage range forward I-V characteristics of Al-BN-nSi (a) Log I. v.s. $\frac{q}{k_B T}$ for different applied voltage, (b) Log I. v.s. $V_G^{\frac{1}{2}}$.

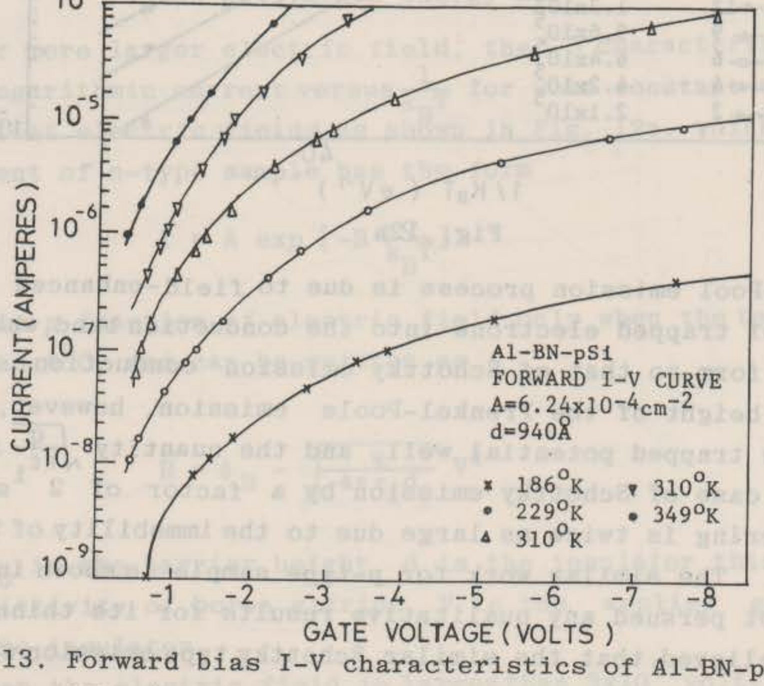

Fig. 13. Forward bias I-V characteristics of Al-BN-pSi MIS structure.

Revese bias current-voltage characteristics for n- and p-type Si samples are shown in Fig. 14 and Fig. 15, respectively. From Fig. 14, the reverse current is much smaller than that of the forward bias of the same type sample, and shows the slow variation with respect to the reverse voltage increasing, which is similar to the case of Schottky barrier lowering reverse current. From previous results of the n-type Si forward bias Schottky emission current, the barrier height for the electron passing through the boron nitride thin film from the conduction band, is only 0.46 ev, the reverse bias of this sample would give a very high barrier of approximate $\phi_{Bp}=$ 2.22 ev (if boron-nitride energy gap is assumed to be 3.8 ev) which is impossible for the hole in the inversion layer to across the insulator. Hence the reverse current will be attributed to the electrons in the metal across the boron nitride by the Schottky emission process, which is slightly increased with the reverse voltage due to the metal-insulator barrier lowering. The similar case would apply for p-type Si sample, if the boron nitride energy gap is known. For higher reverse voltage, the space charge region of both Si n- and p-type sample will breakdown when the electric field in the space charge region is larger than the avalanche limiting electric field strength.

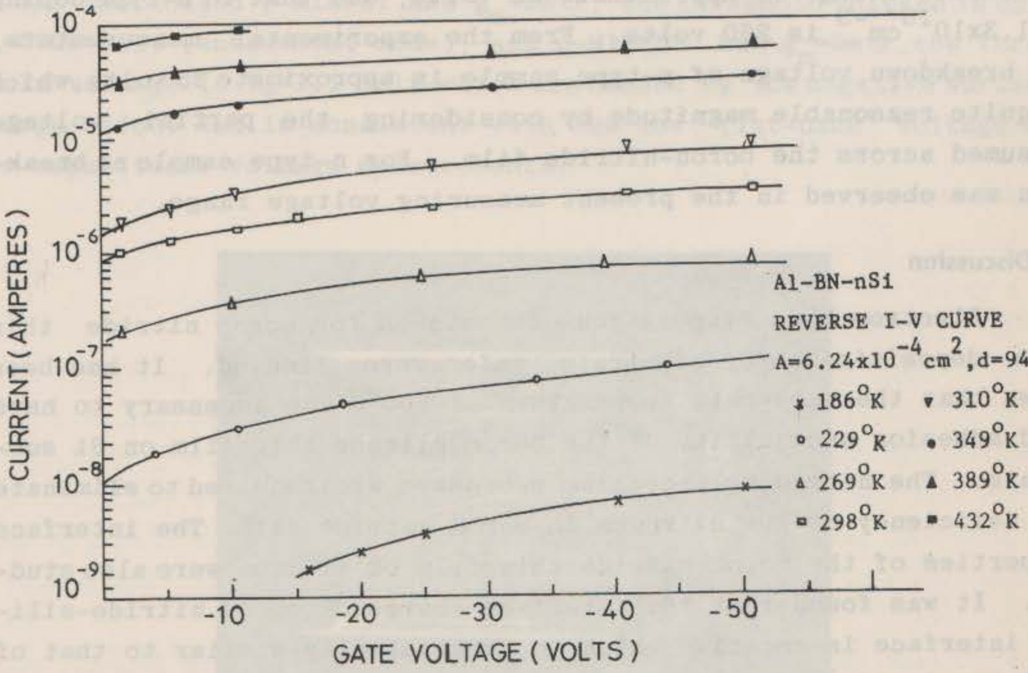

Fig. 14. Reverse bias I-V characteristics of Al-BN-pSi MIS structure.

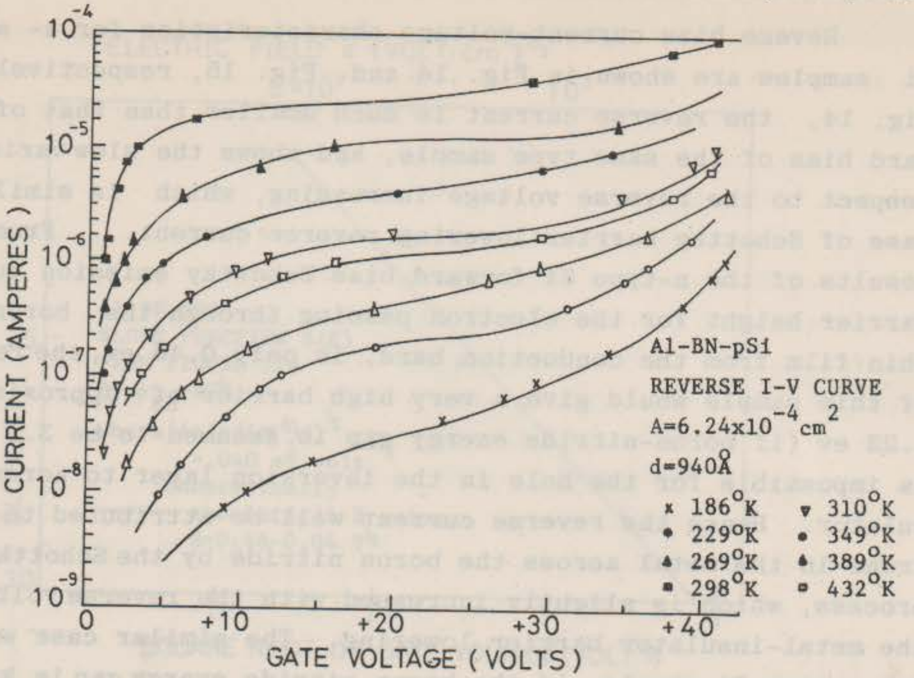

Fig. 15. Reverse bias I-V characteristics of Al-BN-pSi MIS structure.

For our sample, p-type doping of $1.8 \times 10^{16}/cm^3$ will give theoretical breakdown voltage of approximate 32 volts, and that of n-type doping of $1.3 \times 10^{15} cm^{-3}$ is 260 volts. From the experimental measuremtnts, the breakdown voltage of p-type sample is approximate 35 volts, which is quite reasonable magnitude by considering the partial voltage consumed across the boron-nitride film. For n-type sample no breakdown was observed in the present measuring voltage range.

IV. Discussion

Electron beam evaporation techniques for boron nitride thin film deposition on Si substrate wafer were studied. It had been shown that the substrate temperature of 600°C was necessary to have good adhesion and quality of the boron nitride thin film on Si substrate. The nitriding annealing processes are required to eliminate the deficiency of the nitrogen in boron nitride film. The interface properties of the boron nitride thin film on silicon were also studied. It was found that the interface charge of boron nitride-silicon interface is negative which is substantially similar to that of silicon nitride-and aluminum oxide-silicon interfaces, the negative interface charge might be due to the deficiency of the nitrogen atoms attached on the silicon bare surface. The flat-band voltage of boron nitride on Si is smaller than 1 volt and the dielectric constant is 9.3, which is better than those of Si-SiO_2 interface. The dielectric electric field strength of boron nitride is nearly the same as that of SiO_2, but the conductivity of boron nitride is rather larger and is dependent of the annealing condition. The present large electric conductivity of boron nitride thin films might be due to the impurity of B_2O_3 which is a precipitates within the commercial boron nitride diffusion wafer. The boron-oxide impurity on boron-nitride thin film gives the activation energy of only 0.395 ev near the conduction band, which is equivalent to a donor type of impurity state. The donor type of impurity state will spin the fermi-level of the boron nitride above the midgap of boron nitride energy gap, which is self-consistent with the present Schottky emission conduction current flow from the n-type silicon substrate with a barrier height ϕ_{Bn}=0.46 ev in the forward bias gate voltage.

A p- and n-channel MISFET using boron nitride as an insulator layer are fabricated by using the conventional planar technology, except that the insulator layer of boron-nitride is deposited by electron-beam evaporation, which is shown in Fig. 16. The transconductance of the fabricated p-MISFET has g_m=2m℧, the threshold voltage is only V_T=500m volt (enhacement mode), and n-MISFET has g_m=5m℧, the threshold voltage is V_T=1.1 volt which are caused by the negative surface charge effect and is consistent with the low flat-band voltage of our capacitance-voltage measurements.

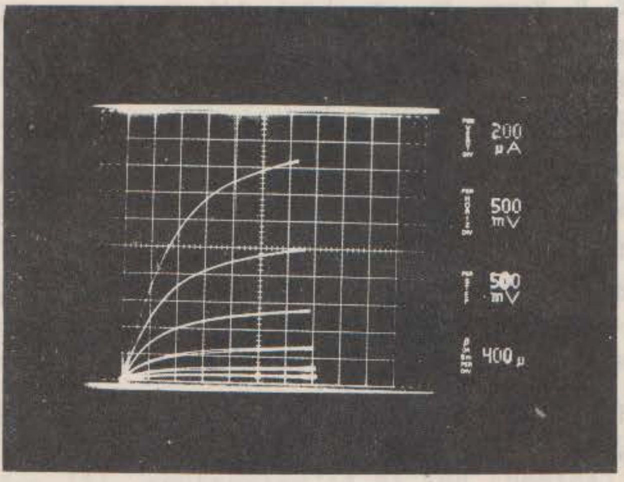

Fig. 16a. p-channel BN gate MIST with V_T=0.5 volt.

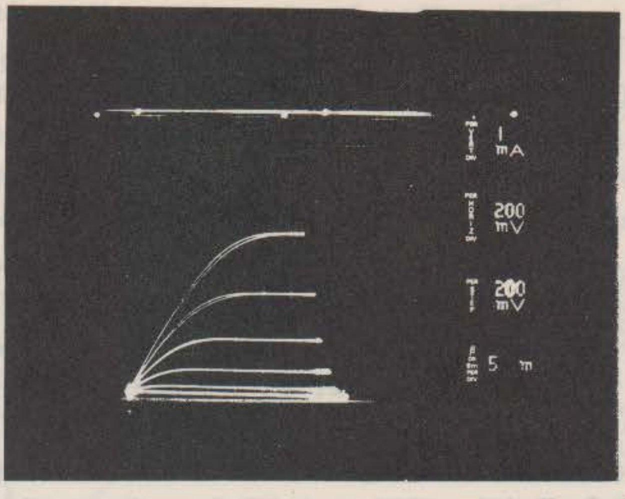

Fig. 16b. n channel BN gate MIST with V_T=1.1 volt.

Fig. 16. I-V characteristics of BN p- and n-channel MISFET.

The gate leakage current is very large when the gate voltage is increased beyond 5 volt and the maximum drain current is limited at 2mA at the maximum gate rating voltage, which is due to Schottky emission of electron across the insulator boron-nitride layer. This gate injection properties can be used as active wave-shaped amplifier circuit to generate the pulse signal. If the low gate injection current is required, the ellimination of the boron oxide impurity contamination is necessary in the boron nitride wafer preparations.

References

1. R. Geick and C. H. Perry, Phy. Rev. Vol. 146, No. 2, pp. 543, 1966.
2. A Katzir, J. T. Suss and A. Zunger, A. Halperin, Phy. Rev. (B) Vol. II, No. 6, pp. 2370, 1975.
3. W. E. Kuhn, Electrochemical Technology, Vol. 4, No. 3-4, pp. 167, 1966.
4. R. J. Patterson, R. D. Humphries, and R. R. Haberecht, Papers presented at the Pittzburgh Meeting of the Society, April 15-18, 1963, Abstract 103, and the New York meeting, Sept. 29-Oct. 3, 1963 as Abstract 197; R. R. Haberecht, R. J. Patterson, and R. R. Humphries, paper presented at the annual Meeting of the Conference on Electrical Insulation, National Research Council, Washington, D. C., 1964.
5. M. J. Rand and J. F. Roberts, J. Electrochem. Soc: Solid State Science, Vol. 115, No. 4, pp. 425, 1968.
6. D. N. Poluboyarinov, N. V. Shishkor and I. G. Kuznetsova, Inorganic Matter, Vol. 3, No. 10, pp. 1828, 1967, USSR.
7. S. M. Sze "Physics of semiconductor devices" pp. 496, 1969.